Linear stability of convective flow in an infinite horizontal layer with horizontal temperature gradient and vertical magnetic field

HUDOBA, A., MOLOKOV, S.,
Department of Mathematics and Physics, Coventry University,
Priory Street, Coventry, CV1 5FB, United Kingdom
E-mail: hudobaa@uni.coventry.ac.uk

The problem of instabilities in the buoyant convective flows subject to high magnetic fields is of particular importance in such industrial applications as fusion reactor blankets, semiconductor crystal growth and electromagnetic processing of materials. In the present study we investigate linear stability of buoyancy-driven convection in a laterally heated layer between two infinite plates subject to a uniform, vertical magnetic field and in the presence of gravity. The mechanisms for different wall conductivities and different values of Hartmann, Ha, and magnetic Prandtl, Pr_m, numbers are investigated. We compare the problem for small, but non-zero Pr_m, with the inductionless approximation in order to determine the validity of that approximation. Linear stability results show that the instability critically depends on the electrical and thermal boundary conditions, and on the Prandtl number, Pr, and on Ha and Pr_m. The instability is driven by different mechanisms depending on these parameters.

1 Problem formulation

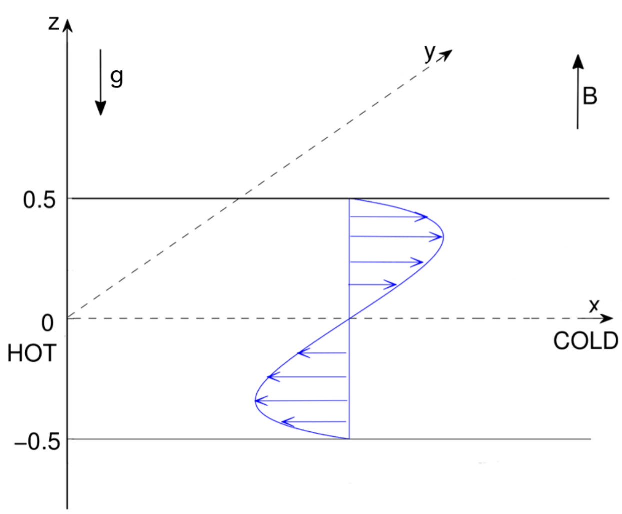

Figure 1. Schematic diagram of the buoyant convective flow with horizontal temperature gradient and a vertical magnetic field

Consider the problem of linear stability of buoyancy-driven convection resulted from axial heating of a fluid layer bounded by infinite horizontal rigid plates, as shown in Fig. 1. The flow, subject to a uniform, vertical magnetic field $\mathbf{B}_0 = B_0\mathbf{e_z}$ is studied in the presence of gravity $\mathbf{g}$. Here (x, y, z) are Cartesian co-ordinates. In a laboratory implementation, two opposite vertical boundaries are set at different temperatures and the horizontal gradient drives the fluid upward near the hot and downward near the cold wall.
The flow is time-dependent, viscous, electrically conducting and incompressible. Material parameters of the fluid are defined by the density ρ, kinematic viscosity ν, thermal conductivity κ, thermal expansion coefficient β and electric conductivity σ. Constant horizontal temperature gradient, which induces a steady circulation, is applied. The top and bottom rigid boundaries of the layer can be either perfectly insulating or perfectly conducting, both thermally and electrically.

2 Governing equations and boundary conditions

The behaviour of the flow is governed by the set of magnetohydrodynamic equations combining Navier-Stokes equations of motion of fluid substances, the energy equation and Maxwell electrodynamics equations. Detailed derivation of these equations has been presented in [1].

The nondimensional form of governing equations results from scaling the length by a reference distance d (the distance between walls), time by d^2/ν, velocity by ν/d, pressure by $\rho\nu^2/d^2$, temperature by ΔT and magnetic field by B_0. Nondimentional Hartmann, Ha, Grashof, Gr, and Prandtl, Pr, numbers are used as control parameters: $Ha = B_0 d\sqrt{\sigma/(\rho\nu)}$, $Gr = g\beta\Delta T(d^4/\nu^2)$, $Pr = \nu/\kappa$, $Pr_m = \mu\sigma\nu$.

The resulting set of nondimensional equations governing the motion of the fluid is:

$$\partial_t \mathbf{v} + (\mathbf{v}\cdot\nabla)\mathbf{v} = -\nabla p + \nabla^2\mathbf{v} + \frac{Ha^2}{Pr_m}(\nabla\times\mathbf{B})\times\mathbf{B} + GrT\hat{e}_z \ , \tag{1}$$

$$\partial_t \mathbf{B} + (\mathbf{v}\cdot\nabla)\mathbf{B} = \frac{1}{Pr_m}\nabla^2\mathbf{B} + (\mathbf{B}\cdot\nabla)\mathbf{v} \ , \qquad \partial_t T + (\mathbf{v}\cdot\nabla)T = \frac{1}{Pr}\nabla^2 T \ , \tag{2),(3}$$

where $\mathbf{v}$, p, $\mathbf{B}$, T are the fluid velocity, pressure, magnetic field and temperature, respectively.

2.1 Basic flow

The problem of buoyant convective flow subject to a vertical magnetic field has a steady mean flow solution [2] with velocity $\mathbf{u}_0 = [u_0(z), 0, 0]$, magnetic field $\mathbf{B} = [b_0(z), 0, 1]$ and temperature $T_0(x, z)$ profiles:

$$u_0 = \frac{Gr}{Ha^2}\left\{z - \frac{\sinh(Haz)}{\sinh(Ha)}\right\} \ , \tag{4}$$

$$b_0 = \frac{Pr_m Gr}{Ha^2}\left\{\frac{\cosh(Haz)}{Ha\sinh(Ha)} - \frac{1}{2}z^2 + \frac{1}{2} - \frac{\cosh(Ha)}{Ha\sinh(Ha)}\right\} \ , \tag{5}$$

$$T_0 = -x + \frac{PrGr}{Ha^2}\left\{\frac{\sinh(Haz)}{Ha^2\sinh(Ha)} - \frac{1}{6}z^3 + Dz\right\} \ , \tag{6}$$

with $D = \frac{1}{6} - \frac{1}{Ha^2}$ for thermally conducting and $D = \frac{1}{2} - \frac{\cosh(Ha)}{Ha\sinh(Ha)}$ for thermally insulating walls.

2.2 Disturbance equations and boundary conditions

In order to test whether the equilibrium state is stable, reaction of the system to small perturbations is examined. The stability is investigated here by the linear analysis. Assuming that disturbances to the flow are fully 3D, the flow can be decomposed into the base flow and the fluctuating component $F = F_0 + \tilde{f}(x, y, z, t)$. Additionally the perturbations can be expressed with Fourier expansions in the $x-$ and $y-$ directions $\tilde{f}(x, y, z, t) = \hat{f}(z)\exp\{ixk_x + iyk_y + \lambda t\}$, where k_x and k_y are the wavenumbers in the $x-$ and $y-$ directions, respectively, and $\lambda = \lambda_r + i\lambda_i$ with real part λ_r representing the growth rate and λ_i an angular oscillation frequency.

Assuming that the introduced perturbation is infinitisemally small, the problem is linearised. Additionally in order to reduce the number of variables the vorticity vector is introduced $\underline{\omega} = \nabla \times \mathbf{v}$. This leads to the following set of equations for the disturbed vorticity, velocity, magnetic field, electric current components, and the disturbed temperature:

$$\{\mathbf{D}^2 - u_0 ik_x\}\hat{\omega}_z + (\partial_z u_0) ik_y \hat{w} + Ha^2\{\partial_z + b_0 ik_x\}\hat{j}_z - \frac{Ha^2}{Pr_m}(\partial_z b_0) ik_y \hat{b}_z = \lambda\hat{\omega}_z \ , \tag{7}$$

$$\{\mathbf{D}^4 - u_0 ik_x \mathbf{D}^2 + (\partial_z^2 u_0) ik_x\}\hat{w} + \frac{Ha^2}{Pr_m}\{+\mathbf{D}^2\partial_z + b_0 ik_x \mathbf{D}^2 - (\partial_z^2 b_0) ik_x\}\hat{b}_z - Grk^2\hat{\theta} = \lambda \mathbf{D}^2 \hat{w} \ , \tag{8}$$

$$\{\frac{1}{Pr_m}\mathbf{D}^2 - u_0 ik_x\}\hat{b}_z + \{b_0 ik_x + \partial_z\}\hat{w} = \lambda \hat{b}_z \ , \tag{9}$$

$$\{\mathbf{D}^2 - Pr_m u_0 ik_x\}\hat{j}_z + \{b_0 ik_x + \partial_z\}\hat{\omega}_z + (\partial_z b_0) ik_y \hat{w} - (\partial_z u_0) ik_y \hat{b}_z = \lambda Pr_m \hat{j}_z \ , \tag{10}$$

$$\{Pr^{-1}\mathbf{D}^2 - u_0 ik_x\}\hat{\theta} - \{\partial_z T_0 + i(\partial_x T_0)\frac{k_x}{k^2}\partial_z\}\hat{w} - i(\partial_x T_0)\frac{k_y}{k^2}\hat{\omega}_z = \lambda\hat{\theta} \ . \tag{11}$$

Here the operator $\mathbf{D} = i\mathbf{k} + [0, 0, \partial z]$ has been introduced.

The appropriate boundary conditions have been applied at the top and bottom rigid boundaries. In the case of thermal and electromagnetic boundary conditions, limit cases are considered here: perfectly conducting or perfectly insulating. These conditions are:

$\hat{\omega}_z = 0$ and $\hat{w} = \partial_z \hat{w} = 0$ at $z = \pm 0.5$,
$\hat{\theta} = 0$ for thermally conducting and $\partial_z \hat{\theta} = 0$ for thermally insulating walls at $z = \pm 0.5$,
$\partial_z \hat{j}_z = 0$ and $\hat{b}_z = 0$ for electrically conducting walls at $z = \pm 0.5$,
$\hat{j}_z = 0$ and $\{\partial_z \pm k\}\hat{b}_z = 0$ for electrically insulating walls at $z = \pm 0.5$.

3 Linear stability results

The problem has been solved numerically by the Chebyshev spectral collocation method and the numerical linear stability results have been obtained. Characteristic lows are given by the critical Grashof number, Gr, (giving the strength of buoyancy forces) as a function of parameters. Beyond those critical values, the basic flow loses its stability. Such neutral stability results have been calculated for fixed values of Pr and Ha, defining $(Gr)_{crit}$ for which an eigenvalue has a real part equal to zero, by minimisation along k_x and k_y.

Here we present the results for the transverse modes ($k_y = 0$) having their axes perpendicular to the main flow. For $Pr_m \to 0$ the electrical boundary conditions show no effect on the transverse instabilities. The magnetic field stabilises these modes very efficiently shifting the onset of instabilities to higher Grashof numbers. The stationary instabilities reach the limiting values at $Ha \simeq 14.5$ for the thermally conducting case and $Ha \simeq 11.5$ for the thermally insulating case, before their disappearance (Figs. 2 and 3). The wavenumbers are slowly decreasing with Ha until reaching the minima just before the disappearance of these modes. At the higher values of Ha, instabilities appear mainly as a result of potentially unstable thermal stratification zones near the horizontal boundaries and exist only for thermally conducting cases.

The inductionless approximation is confirmed to be valid for Pr_m up to $Pr_m = 10^{-4}$ for the range of Ha considered here. An increase of the value of Pr_m results in a divergence between the two cases of electromagnetic boundary conditions.

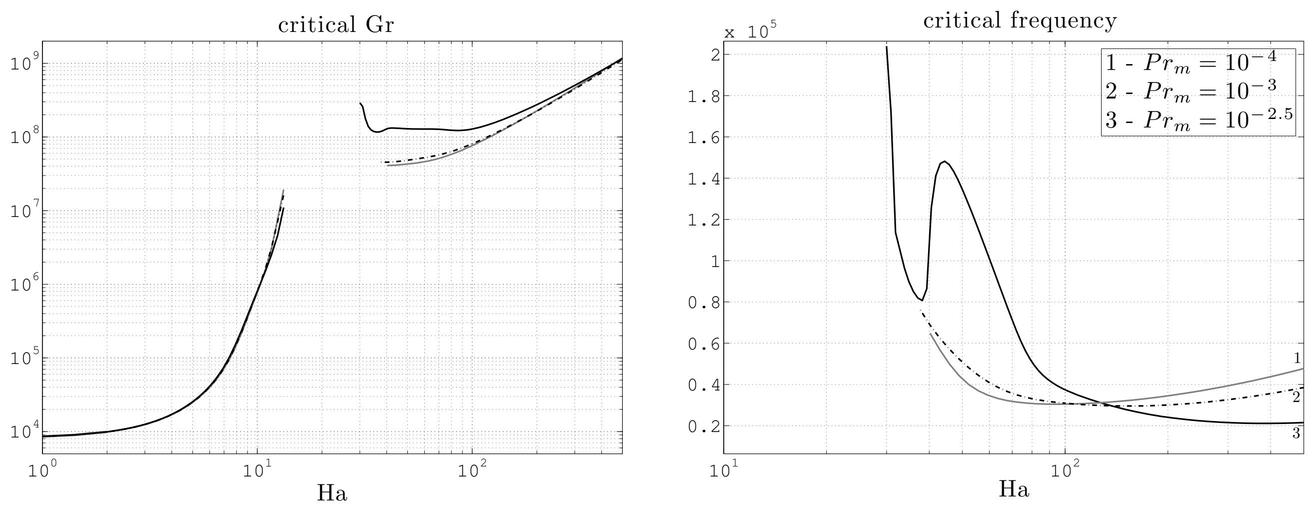

Figure 2. Critical values of parameters, thermally & electrically conducting walls

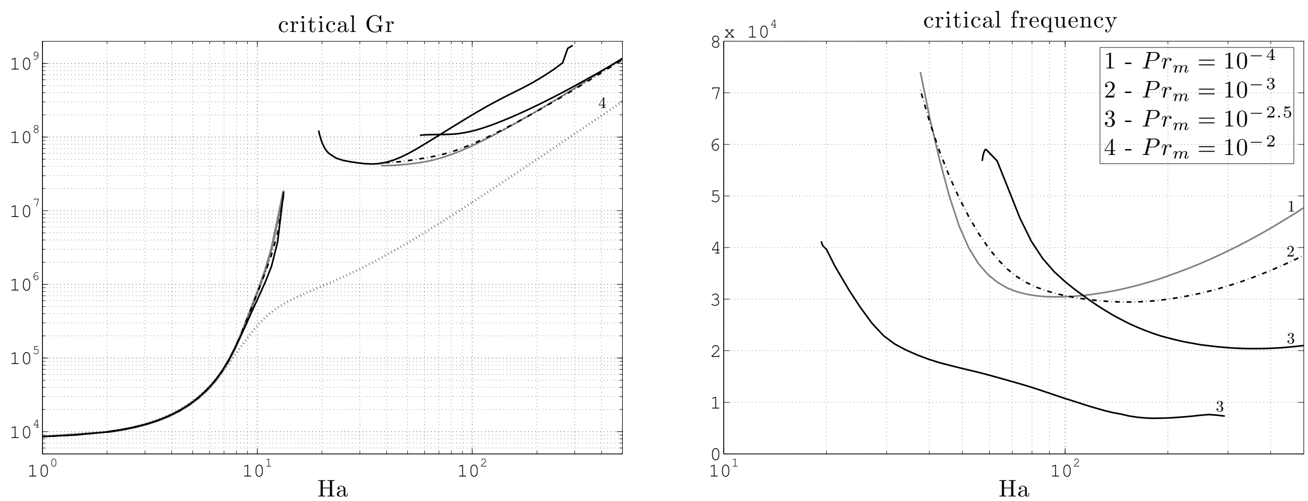

Figure 3. Critical values of parameters, thermally conducting & electrically insulating walls.

The stationary branches, for all the boundary conditions, lie very closely to one another for different magnetic Prandtl numbers, with the lower Pr_m modes disappearing at slightly lower Ha values. The wavenumber decreases with the increasing Pr_m, which is apparent for the thermally insulating cases (Figs. 4 and 5; notice that all the modes in these figures are stationary). The increase of Pr_m number has a stabilising effect on thermal oscillatory branches for both cases of electromagnetic boundary conditions (Figs. 2 and 3). The osciallatory instabilities appear at higher frequencies for the higher Pr_m, while the wavenumbers decrease causing the increase of the marginal cells.

We observed new branches of instabilities for the cases of electrically insulating walls (Figs. 3 and 5). The new modes appearing at higher Ha in the case of thermally conducting boundaries are more stable (Fig.3), with low wavenumbers and relatively low frequencies. The new stationary instabilities, appearing for both thermally conducting and insulating boundaries, become the most dangerous modes (Figs. 3 and 5).

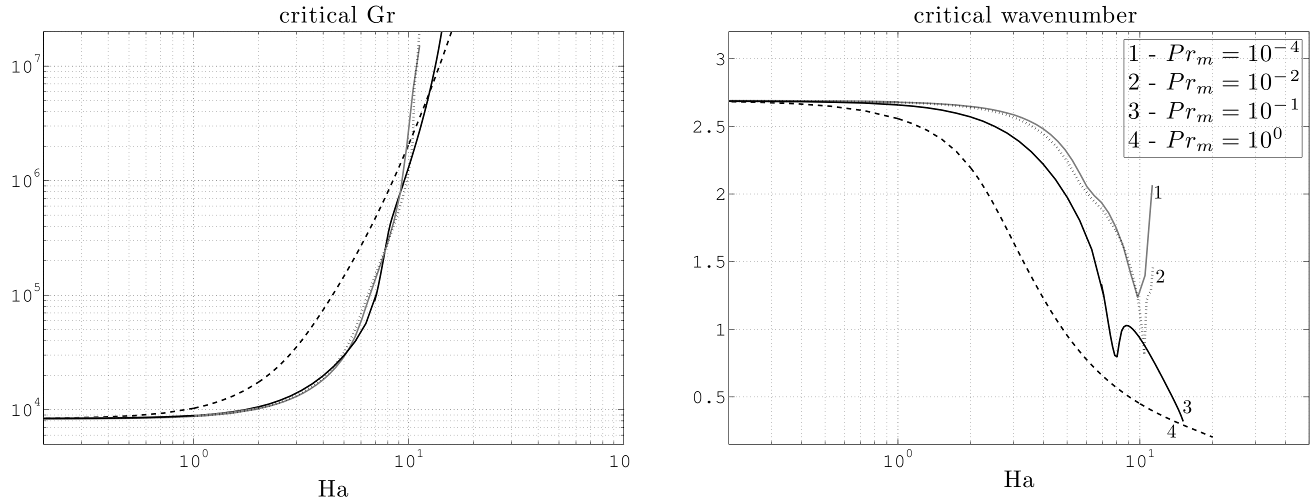

Figure 4. Critical values of parameters, thermally insulating & electrically conducting walls.

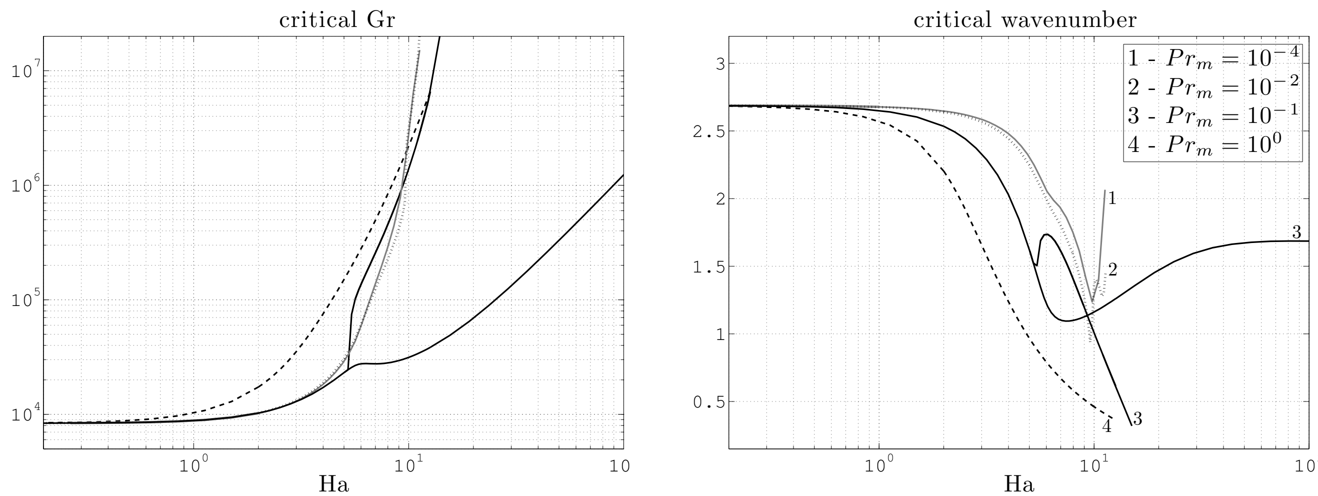

Figure 5. Critical values of parameters, thermally insulating & electrically insulating walls

4 Conclusions

The results show that the inductionless approximation is valid for the values of Pr_m up to $Pr_m = 10^{-4}$ for the range of Ha considered here. Further increase of Pr_m will cause a divergence between different modes, depending on the boundary conditions, and on the values of critical parameters. For the case of electrically insulating boundaries there are new most dangerous instabilities appearing for the whole range of Ha. The detailed results of this investigation, together with the results for the longitudinal modes will be discussed in a full journal paper.

References

[1] Muller, U.; Buhler, L.: Magnetofluiddynamics in channels and containers. Springer, 2001.

[2] Priede, J.; Aleksandrova, S.; Molokov, S.: Stability of buoyant convection in laterally heated liquid metal layer subject to transverse magnetic field. Proc. of the 7th PAMIR Conference, France, 2008

[3] Lappa, M.: Thermal convection. Patterns, evolution and stability. John Wiley & Sons, 2010.

[4] Kaddeche, S.; Henry,D.; BenHadid, H.: J. Fluid Mech. 480 (2003) 185-216